

RESEARCH

Open Access



PTPN20 promotes metastasis through activating NF- κ B signaling in triple-negative breast cancer

Xiaoxiao Zuo^{1,3†}, Xiaohan Zhao^{2†}, Xiaofei Zhang^{4†}, Qingyuan Li^{5†}, Xingyu Jiang², Shumei Huang⁶, Xuwei Chen², Xiangfu Chen², Weihua Jia^{2,7}, Hequn Zou^{5*}, Dongni Shi^{2*} and Xueke Qian^{1*}

Abstract

Background Cancer metastasis remains a major challenge in the clinical management of triple-negative breast cancer (TNBC). The NF- κ B signaling pathway has been implicated as a crucial factor in the development of metastases, but the underlying molecular mechanisms remain largely unclear.

Methods PTPN20 expression was evaluated using data from the Sweden Cancerome Analysis Network-Breast and The Cancer Genome Atlas database, as well as by western blotting and immunohistochemistry in 88 TNBC patients. The ability of PTPN20 to activate NF- κ B was assessed by luciferase reporter assays. The effects of PTPN20 overexpression and knockdown via short hairpin RNA were examined in TNBC cell lines by wound healing and transwell matrix penetration assays. Additionally, we analyzed the growth and metastasis ability of 4T1 xenograft tumors in nude mice.

Results PTPN20 levels were elevated in TNBC cell lines and patient samples compared to controls, and higher protein levels correlated with metastasis-free survival. Overexpression of PTPN20 enhanced migration and invasion in vitro, and promoted lung metastasis in vivo. Our finding revealed that PTPN20 activates NF- κ B signaling by dephosphorylating p65 at Ser468, preventing its binding to COMMD1, thereby protecting p65 from degradation. Downregulation of PTPN20 effectively inhibit, while p65 S468A mutant restored the migratory and invasive abilities of TNBC cells.

Conclusions Collectively, our results demonstrate that PTPN20 plays a critical role in TNBC metastasis through the activation of NF- κ B signaling. We propose that PTPN20 may serve as a novel prognostic marker and potential therapeutic target for the treatment of TNBC.

[†]Xiaoxiao Zuo, Xiaohan Zhao, Xiaofei Zhang and Qingyuan Li contributed equally to this work.

*Correspondence:

Hequn Zou
zouhequn@cuhk.edu.cn
Dongni Shi
shidn@sysucc.org.cn
Xueke Qian
qxuek@mail3.sysu.edu.cn

Full list of author information is available at the end of the article



© The Author(s) 2024. **Open Access** This article is licensed under a Creative Commons Attribution-NonCommercial-NoDerivatives 4.0 International License, which permits any non-commercial use, sharing, distribution and reproduction in any medium or format, as long as you give appropriate credit to the original author(s) and the source, provide a link to the Creative Commons licence, and indicate if you modified the licensed material. You do not have permission under this licence to share adapted material derived from this article or parts of it. The images or other third party material in this article are included in the article's Creative Commons licence, unless indicated otherwise in a credit line to the material. If material is not included in the article's Creative Commons licence and your intended use is not permitted by statutory regulation or exceeds the permitted use, you will need to obtain permission directly from the copyright holder. To view a copy of this licence, visit <http://creativecommons.org/licenses/by-nc-nd/4.0/>.

Highlights

- The expression of PTPN20 was upregulated specially in triple-negative breast cancer.
- PTPN20 induces metastasis by promoting cell migration and invasion.
- PTPN20 dephosphorylates p65 and activates NF- κ B signaling.
- PTPN20 may be a novel prognostic marker and a potential therapeutic target in the treatment of TNBC.

Keywords PTPN20, TNBC, p65, metastasis

Background

Breast cancer is the second most commonly diagnosed malignancy worldwide and the leading cause of cancer-related mortality in females [1]. Distant metastasis is the primary cause of death in breast cancer patients. Triple-negative breast cancer (TNBC), characterized by the lack of expression of estrogen receptor (ER), progesterone receptor (PR), and human epidermal growth factor-2 (HER2) as determined by immunohistochemistry, accounts for 15–20% of overall breast cancer cases [2–4]. TNBC is considered the most aggressive subtype, with a five-year overall survival rate of less than 80%, compared to approximately 93% for other subtypes [5–7]. TNBC predominantly affects younger women, is poorly differentiated, and carries a high risk of visceral metastases, particularly to the lungs, liver, bones, and brain [7, 8]. Notably, while the local recurrence rates are relatively similar among breast cancer subtypes, the distant metastatic rate in TNBC is significantly higher compared to luminal and HER2-positive subtypes. Furthermore, TNBC is both biologically and clinically heterogeneous, with chemotherapy remaining the cornerstone of systemic treatment. However, there is a critical unmet need for more effective disease control strategies [8, 9]. Therefore, it is imperative to further elucidate the mechanisms of disease progression and distant metastasis in TNBC, and explore novel druggable targets for TNBC treatment.

Hyperactivation of nuclear factor kappa B (NF- κ B) signaling has been implicated in cancer metastasis through the upregulation of multiple factors, such as macrophage colony-stimulating factor (CSF1), granulocyte-macrophage colony-stimulating factor (CSF3), and MMP9 [10–12]. Studies have shown that systemic inhibition of NF- κ B activity significantly reduces breast cancer bone metastasis in vivo, highlighting the critical role of NF- κ B signaling in cancer progression [12]. The NF- κ B transcription factor generally exists as a heterodimer of the p50 and RelA (p65) polypeptides bound in the cytoplasm by the inhibitor protein I κ B [13–15]. Following cellular stimulation, I κ B is phosphorylated and then degraded by the proteasome, allowing NF- κ B to translocate to the nucleus and regulate the expression of downstream genes [16]. Canonical NF- κ B activation triggers a signalling cascade that leads to the phosphorylation of I κ B, and its subsequent ubiquitination and proteasomal elimination [17].

Several mechanisms mediate further layers of NF- κ B regulation, including the post-translational modification of the DNA-binding subunits by phosphorylation, acetylation and ubiquitination. Post-translational modifications, particularly phosphorylation of the p65, are essential for cytoplasmic to nuclear localization of NF- κ B/p65 and initiation of transcription of downstream target genes [18–20]. Phosphorylation of p65 is essential for protein stability and cytoplasmic to nuclear localization of p65, thus determining the initiation of transcription of downstream target genes. Importantly, phosphorylated p65 at Ser468 (p-p65 Ser468) has been shown to undergo ubiquitination and degradation by COMM domain-containing 1 (COMMD1)-complex, thus allowing termination of the nuclear NF- κ B response [21, 22]. However, the regulate mechanism of activating p65/NF- κ B remains unclear.

The protein tyrosine phosphatase (PTP) families plays an integral role in many aspects of cellular signalling and controls diverse fundamental cellular responses, including growth, proliferation, differentiation, migration and immune response [23–26]. PTPN20 is a classical member of PTP families and has been reported that associated with PTPN20 include esophageal carcinoma, gastric cancer and congenital hydrocephalus [27–29]. PTPN20 is a good candidate for prognosing *Helicobacter pylori* (Hp) -related gastric cancer patients and PTPN20 was found to be tightly related to the function of many innate immune cells [28]. However, the role of PTPN20 in the metastasis of TNBC requires further investigation.

In this study, we investigated the role of PTPN20, a member of the protein tyrosine phosphatase (PTP) families, in the metastasis of TNBC. Our study demonstrated that overexpressing of PTPN20 contributed to TNBC metastasis by activating NF- κ B signaling. Specifically, we revealed that PTPN20 dephosphorylates p65 at Ser468, preventing its binding to COMMD1, thus protecting p65 from degradation. These findings highlight the pivotal role of PTPN20 in TNBC metastasis and suggest that it may serve as a promising therapeutic target for TNBC treatment.

Materials and methods

Tissues and cells

A total of 88 paraffin-embedded breast cancer specimens were collected for this study, which had been histopathologically diagnosed at the Sun Yat-sen University

Cancer Center. The fresh breast cancer tissues, including non-TNBCs and TNBCs, and matched adjacent non-tumor breast tissues from the same patient were frozen and stored in liquid nitrogen until required. The approval from the Institutional Research Ethics Committee and donors' consents were obtained.

Breast cancer cell lines MDA-MB-415, MDA-MB-453, MDA-MB-231, MDA-MB-468 and normal breast epithelial cell line MCF10A were cultured in Leibovitz's L-15 Medium with 10% foetal bovine serum (FBS); MCF-7 was cultured in Eagle's Minimum Essential Medium with 10% FBS; ZR-75-1, BT-549, and HCC1937 were cultured in RPMI 1640 with 10% FBS. The above cell lines were purchased from American Type Culture Collection (ATCC, Manassas, VA, USA). SUM159PT was purchased from Aster and Bioscience (Royston, UK) and cultured in Ham's F-12 with 5% FBS, 1 µg/ml hydrocortisone, 5 µg/ml insulin and 10 mM HEPES. All cell lines were incubated at 37 °C in 5% CO₂. All cell lines were authenticated using short tandem repeat (STR) profiling.

Immunohistochemistry

Immunohistochemistry (IHC) analysis was performed on the 88 paraffin-embedded breast cancer tissue sections and 14 non-tumor breast tissues using Histostain-PlusKits (Invitrogen, Carlsbad, CA) following the manufacturer's protocols. An anti-PTPN20 rabbit polyclonal antibody (1:500 dilution, Cat#HPA069148, Sigma-Aldrich) were used for IHC staining. The degree of immunostaining was evaluated and scored by two independent pathologists blinded to the clinical outcome, based on both the proportion of positively stained tumor cells and the intensity of staining. Scores representing positive tumor cell proportions were determined as 0, no positive cells; 1, <10% positive cells; 2, 10–35% positive cells; 3, 35–75% positive cells; 4, >75% positive cells. Staining intensity was graded as following: 0, no staining; 1, weak staining; 2, moderate staining; 3, strong staining. The staining index (SI) was calculated based on both the staining intensity score and the proportion of positive cells, resulting in possible scores of 0, 1, 2, 3, 4, 6, 8, 9 and 12. The SI 4 was defined as the optimal cutoff, and tumors with SI ≥ 4 were defined as high expression, the others were considered as PTPN20-low.

Plasmids and oligonucleotides

The open reading frame (ORF) sequences of PTPN20 were cloned into the pMSCV-puro-retro vector (Clontech, Beijing, China). The short hairpin RNA (shRNA) oligonucleotides targeting PTPN20-3'UTR in pLKO.1-puro vector were purchased (Transheep Bio, Shanghai, China). Luciferase cDNA was PCR-amplified and cloned into the pMSCV-neo-retro vector (Clontech, Beijing, China). Cells (1×10^5) were seeded and infected

by retrovirus generated by pMSCV-puro-cDNAs or lentivirus by pLKO.1-puro shRNAs for 3 days. All cells were further infected with pMSCV-neo-luciferase retrovirus. The stable cell lines were selected with 0.5 µg/mL puromycin and 250 µg/mL G418 for 7 days.

The shRNA sequences targeting PTPN20-3'UTR was as following: PTPN20-shRNA#1: CCACCCTAACAC TTAACATAT. Retroviral production was performed in 293T cells. Stable cell lines expressing PTPN20 ORF and/or PTPN20 shRNA were selected for 10 days with 0.5 µg/mL puromycin 48 h after infection. After 10-day selections, the cell lysates prepared from the pooled population of cells in sample buffer were fractionated on SDS-PAGE for the detection of PTPN20 protein level.

Western blotting

Cells were harvested in cell lysis buffer (Cell Signaling Technology, Cat#9803) and heated for 5 min at 100 °C. Equal quantities of denatured protein samples were resolved on 10% SDS-polyacrylamide gels, and then transferred onto polyvinylidene difluoride membranes (Roche). Protein concentration was determined with the bicinchoninic acid (BCA) assay (Pierce, Rockford, USA) according to the manufacturer's instructions. After blocking with 5% non-fat dry milk in Tris-buffered saline/0.05% Tween 20 (TBST), the membrane was incubated with a specific primary antibody, followed by the horseradixh peroxidase-conjugated secondary antibody. Proteins were visualized using ECL reagents (Pierce). The anti-PTPN20 (1:1000 dilution, Cat#LS-C406705, LS Bio), anti-p65 (1:1000 dilution, Cat#ab32536, Abcam), anti-p65-Ser468 (1:1000 dilution, Cat#ab264271, Abcam), anti-p65-Ser536 (1:1000 dilution, Cat#ab76302, Abcam), anti-IKKβ (1:1000 dilution, Cat#ab264239, Abcam), anti-p-IKKα/β (p-Ser176/180 of IKKα and pSer177/181 of IKKβ, 1:500 dilution, Cat#2697, CST), anti-IKKα (1:1000 dilution, Cat#ab109749, Abcam), anti-HA (1:1000 dilution, Cat#ab137838, Abcam), anti-Flag (1:1000 dilution, Cat#ab1162, Abcam), anti-IκBα (1:1000 dilution, Cat#ab32518, Abcam), anti-p-IκBα (1:1000 dilution, Cat#9246, CST), anti-H3 (1:1000 dilution, Cat#ab1791, Abcam), anti-GAPDH (1:2000 dilution, Cat#10494-1-AP, Proteintech).

Real-time PCR

Total RNA was extracted from the indicated cells using the Trizol (Life Technologies, Carlsbad, CA, USA) reagent according to the manufacturer's instruction. Quantitative Real-time reverse transcription-polymerase chain reaction (PCR) primers and probes were designed with the assistance of the Primer Express v 2.0 software (Applied Biosystems, Foster City, CA, USA). Expression data were normalized to the geometric mean of housekeeping gene GAPDH to control the variability in expression levels and

calculated as $2^{[(Ct \text{ of gene}) - (Ct \text{ of GAPDH})]}$, where Ct represents the cycle threshold for each transcript.

The primers used are as following: PTPN20-up, GAA GAGACAGGTGGAGCAGTGA; PTPN20-dn, GCCG AATCTGAGCCAACCTGATC; TWIST-up, GCCAGGT ACATCGACTTCCTCT; TWIST-dn, TCCATCCTCC AGACCGAGAAGG; CSF1-up, TGAGACACCTCTCC AGTTGCTG; CSF1-dn, GCAATCAGGCTTGGTCAC CACA; CSF3-up, GCAATCAGGCTTGGTCACCACA; CSF3-dn, CGCTATGGAGTTGGCTCAAGCA; CXCL1-up, AGCTTGCCTCAATCCTGCATCC; CXCL1-dn, T CCTTCAGGAACAGCCACCAGT; IL11-up, GGACCA CAACCTGGATTCCCTG; IL11-dn, AGTAGGTCCGC TCGCAGCCTT; MMP9-up, GCCACTACTGTGCCT TTGAGTC; MMP9-dn, CCCTCAGAGAATCGCCAG TACT; GAPDH-up, AAGGTGAAGGTCGGAGTCAA; GAPDH-dn, AATGAAGGGGTCATTGATGG.

Wound healing assay

Cells were seeded on six-well plates with medium containing 10% fetal bovine serum (FBS) and grown to confluence. The cells were scratched with a sterile 200- μ L pipette tip to create artificial wounds. At 0 and 24 h after wounding, phase-contrast images of the wound healing process were photographed with a 10 \times objective lens. Eight images per treatment were analyzed to determine averaging position of the migrating cells at the wound edges.

Transwell matrix penetration assay

Cells (1×10^4) to be tested were plated on the top side of polycarbonate transwell filter (with Matrigel) in the upper chamber of the BioCoatTM Invasion Chambers (BD, Bedford, MA) and incubated at 37 $^\circ$ C for 24 h. Invaded cells on the lower membrane surface were fixed in 1% paraformaldehyde, stained with crystal violet, and counted (Ten random 100 \times fields per well). Three independent experiments were performed and the data are presented as mean \pm standard deviation (SD).

Luciferase assays

Cells (1×10^4) were seeded in triplicate in 48-well plates and allowed to settle for 24 h. One hundred nanograms of luciferase reporter plasmids or the control-luciferase plasmid, plus 5 ng of pRL-TK renilla plasmid (Promega, Madison, WI), were transfected into indicated cells using the Lipofectamine 3000 reagent (Invitrogen, Carlsbad, CA, USA) according to the manufacturer's recommendation. Luciferase and renilla signals were measured at 48 h after transfection using the Dual Luciferase Reporter Assay Kit (Promega, Madison, WI) according to a protocol provided by the manufacturer.

Immunoprecipitation (IP) assay

Cells grown in 100-mm culture dishes were lysed using 500 μ L of lysis buffer (25 mM HEPES, 150 mM NaCl, 1% NP-40, 1 mM EDTA, 2% glycerol, 1 mM phenylmethylsulfonyl fluoride). After being maintained on ice for 30 min, the lysates were clarified by microcentrifugation at 12,000 rpm for 10 min. To preclear the supernatants, the lysates were incubated with 20 μ L of agarose beads (Calbiochem, Cambridge, MA) for 1 h with rotation at 4 $^\circ$ C. After centrifugation at 2,000 rpm for 1 min, the supernatants were incubated with 20 μ L of antibody-cross-linked protein G-agarose beads overnight at 4 $^\circ$ C. The agarose beads were then washed six times with wash buffer (25 mM HEPES, 150 mM NaCl, 0.5% NP-40, 1 mM EDTA, 2% glycerol, 1 mM PMSF). After removing all the liquid, the pelleted beads were resuspended in 30 μ L of 1 M glycine, after which 10 μ L of 4 \times sample buffer was added, the samples were denatured, and the sample components were electrophoretically separated on SDS-polyacrylamide gels for western blotting analysis.

In vitro phosphatase assays

Each anti-FLAG bead-bound protein was mixed in 20 μ L PTP reaction buffer (100 mM Tris-HCl (pH 7.5), 40 mM NaCl, and 1 mM DTT) and reaction mixtures were incubated at 30 $^\circ$ C for 30 min. CIP was used to prove the bands detected by each antibody, which recognizes specific phosphorylation sites, are phosphospecific bands. Phosphatase reaction was stopped by adding 5 \times sample buffer. The beads were then resolved on SDS-PAGE and analyzed by immunoblotting using specific antibodies.

Xenograft models

All experimental procedures were approved by the Institutional Animal Care and Use Committee of Sun Yat-sen University, and complied with the Guidelines for the Welfare and Use of Animals. Female BALB/c-nude mice (5 weeks old, 18–20 g) were purchased from the Slac-Jingda Animal Laboratory (Hunan, China), and housed in barrier facilities on a 12 h light/dark cycle. The mice were randomly divided into groups ($n=6$ /group). To test the tumorigenicity, mice were inoculated subcutaneously with 5×10^6 cells in the mammary fat pad. Seven days later, kinetics of tumor formation was estimated by measuring tumor volume every 3 days. Tumor volume was calculated using the equation $(L \times W^2)/2$. Six weeks later, tumors were detected by an IVIS imaging system (Caliper), and tumors were excised and weighed. In the lung colonization model, mice were intravenously injected with control or indicated cells. Lung metastases were determined 5 weeks post injection of 1×10^5 cells. The number of lung tumor nests in each group was counted under five random low power field and presented as the mean \pm standard deviation (SD).

Statistical analysis

Statistical analysis was performed using the GraphPad Prism 8 and SPSS 21.0 statistical software. Student's t-test, Kruskal-Wallis test and Mann-whitney U test were used for the compare of continuous data. Survival curves were plotted with the Kaplan-Meier method and compared by the log-rank test. *P*-values of 0.05 or less were considered statistically significant. All data were presented as the mean ± standard deviation (SD). Representation of the *P*-value was **P* < 0.05, ***P* < 0.01, ****P* < 0.001.

Results

PTPN20 is upregulated especially in TNBC

To investigate the role of PTPN20 in TNBC, we analyzed its expression using data from the Sweden Cancerome Analysis Network-Breast (SCAN-B) dataset, which includes GSE96058 and GSE81538, as well as The Cancer Genome Atlas (TCGA) database [30, 31]. PTPN20 was found to be overexpressed in both basal-like and TNBC patients, according to Parker's intrinsic molecular subtypes and immunohistochemical analysis of ER, HER2, and PR in the SCAN-B dataset (Fig. 1A). Similarly, TCGA data analysis revealed elevated PTPN20 expression in TNBC patients based on immunohistochemistry (Fig. 1B). Additionally, PTPN20 expression was significantly higher in the TNBC-M (Mesenchymal like) subtype compared to other groups based on a unique gene expression signature (Fig. 1C), suggesting that patients with high PTPN20 expression may have a greater propensity for metastasis [32, 33]. Furthermore, we examined the mRNA and protein expression of PTPN20 in 10 breast cell lines, including 1 normal breast epithelial cell, 4 non-TNBC cell lines and 5 TNBC cell lines, by Real-time PCR and western blotting respectively. We found that PTPN20 was overexpressed particularly in TNBC cell lines (including MDA-MB-468, SUM159PT, BT549, HCC1937 and MDA-MB-231) (Fig. 1D). Moreover, PTPN20 expression at both the mRNA and protein levels was upregulated in TNBC tissues compared to non-TNBC tissues (Fig. 1E). Dramatically, the expression of PTPN20 was upregulated in breast cancer tissues, and further elevated in those with 5-year metastasis (Fig. 1F). Correlation analysis revealed that high expression of PTPN20 positively and significantly correlated with metastatic relapse in patients (Fig. 1G). Taken together, these findings indicated that overexpression of PTPN20 might contribute to TNBC metastasis.

PTPN20 enhances the metastatic ability of TNBC cells

To evaluate the effect of PTPN20 on the metastatic potential of TNBC cells, we established cell lines stably expressing PTPN20 shRNA, with or without the open reading frame (ORF) of PTPN20, and confirmed PTPN20 expression (Fig. 2A). We then performed wound-healing

and transwell invasion assays in TNBC cells. Silencing PTPN20 significantly reduced the migratory and invasive capabilities of TNBC cells, while reintroducing PTPN20 restored these abilities in the PTPN20-silenced cells (Fig. 2B-C). Additionally, overexpression of PTPN20 enhanced the migration and invasive ability (Fig. 2D-F).

Next, we investigated whether PTPN20 promotes TNBC aggressiveness in vivo. Knockdown of PTPN20 markedly inhibited tumor growth rate and tumor weight compared to the control group, whereas overexpression of PTPN20 accelerated tumor growth (Fig. 2G-I). Furthermore, we assessed the effects of PTPN20 on breast cancer metastasis using a lung colonization model. PTPN20-overexpressing cells were injected into BALB/c nude mice via the lateral tail vein and metastatic activity was examined by bioluminescence imaging (BLI) of luciferase-transduced cells. Knockdown of PTPN20 significantly reduced lung metastasis, whereas overexpression of PTPN20 increased the metastatic burden (Fig. 2J-K). Importantly, knockdown of PTPN20 decreased the metastatic index, while its overexpression conversely increased the metastatic index (Fig. 2L). These findings suggested that PTPN20 enhances the metastatic ability of TNBC.

PTPN20 activates p65/NF-κB signaling pathway in TNBC cells

To further elucidate the mechanism underlying PTPN20-mediated metastasis, we performed a Cignal Finder 45-pathway reporter array in vector- and PTPN20-transduced MDA-MB-231 cells. Notably, the NF-κB transcriptional activity was most significantly induced in PTPN20-overexpressing cells compared to vector cells (Fig. 3A-B), suggesting that PTPN20 may be involved in the modulation of the NF-κB pathway. Consistent with this hypothesis, overexpression of PTPN20 markedly increased NF-κB luciferase activity (Fig. 3C). Furthermore, restoring PTPN20 expression enhanced NF-κB luciferase activity in PTPN20-silenced cells (Fig. 3D). In agreement with these results, overexpression of PTPN20 upregulated, whereas knockdown of PTPN20 inhibited NF-κB response gene expression (Fig. 3E-G). These findings suggested that PTPN20 overexpression activates the NF-κB pathway in TNBC cells.

To investigate the mechanism underlying PTPN20-mediated NF-κB activation, we examined the effect of PTPN20 in NF-κB-related factors. Notably, PTPN20 specifically decreased phosphorylation of p65 at the Ser468 site while increasing total p65 levels, without affecting most other factors, including p-IKKα/β, p-IκBα or p-p65 (Ser536) (Fig. 3H). It is known that phosphorylation of p65 at Ser468 leads to ubiquitin/proteasome-dependent removal of chromatin-bound p65, thus contributing to the selective termination of

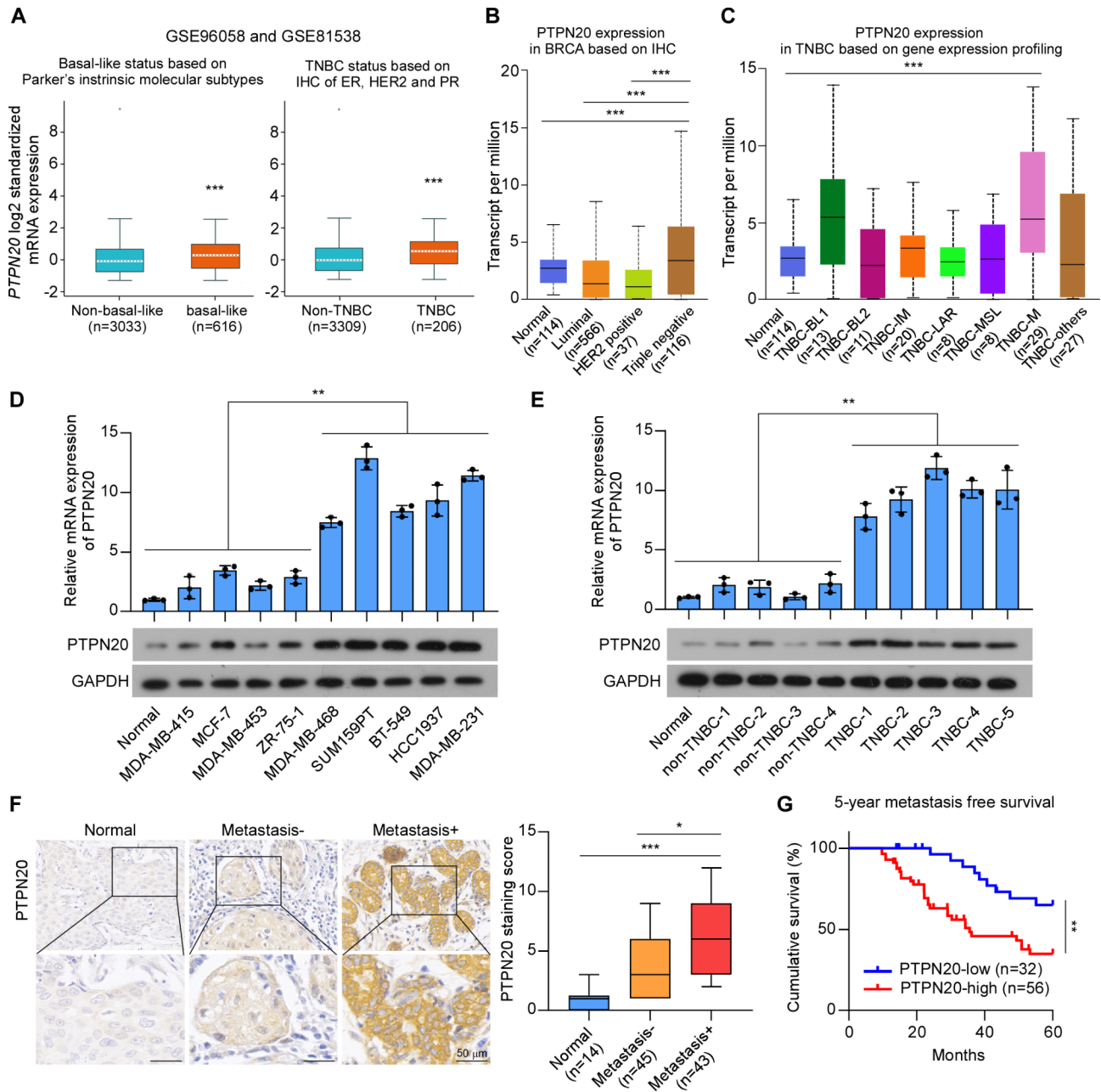


Fig. 1 PTPN20 is upregulated especially in TNBC. **(A)** PTPN20 mRNA expression levels from the Sweden Cancerome Analysis Network-Breast dataset (SCAN-B, including GSE96058 and GSE81538). The basal-like status was identified based on Parker's intrinsic molecular subtypes, and the TNBC status was identified based on means of ER, HER2, and PR expression by IHC. **(B)** PTPN20 mRNA expression levels in The Cancer Genome Atlas (TCGA) breast cancer dataset including 114 normal, 566 Luminal, 37 HER2 positive and 116 Triple negative samples. The subtypes were classified based on means of ER, HER2, and PR expression by IHC. **(C)** PTPN20 mRNA expression levels in tumor samples with informed molecular subtypes from TCGA breast cancer dataset. Statistic analysis was normalized to the expression levels in Normal subgroup. BL1, Basal like 1; BL2, Basal like 2; IM, Immunomodulatory; LAR, luminal androgen receptor; MSL, mesenchymal stem-like; M, Mesenchymal. The six TNBC subtypes were categorized by gene expression profiling. **(D)** Real-time PCR (up) and western blotting (down) analysis of PTPN20 expression in cells including 1 normal breast epithelial cell, 4 non-TNBC cell lines (MDA-MB-415, MCF-7, MDA-MB-453 and ZR-75-1) and 5 TNBC cell lines (MDA-MB-468, SUM159PT, BT549, HCC1937 and MDA-MB-231). **(E)** Real-time PCR (up) and western blotting (down) analysis of PTPN20 expression in normal breast tissues and human breast cancer tissues. GAPDH was used as a loading control. **(F)** Representative photomicrographs (left) and the staining index (right) of PTPN20 in normal (n = 14) and tumor specimens with (n = 43) or without metastatic relapse (n = 45) in 5 years. **(G)** Correlation between 5-year metastatic relapse and PTPN20 expression in patients. Log-rank test was used. In (D) and (E), error bars represent the mean ± SD of three independent experiments. In (A), (B) and (C), Welch-test was used. In (D) and (E), Mann-Whitney U test was used. In (F), Kruskal-Wallis test was used. ***P < 0.001, **P < 0.01, *P < 0.05

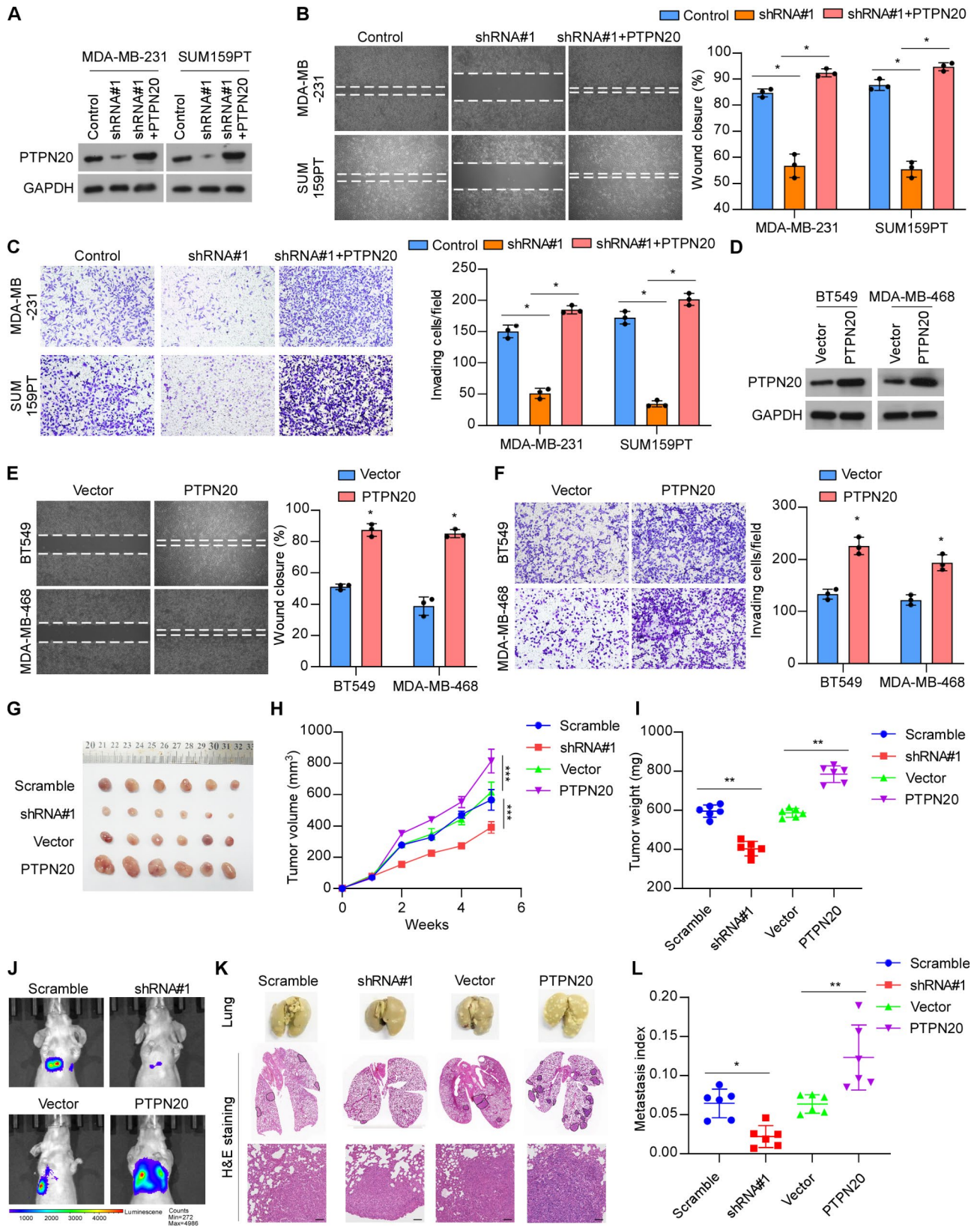


Fig. 2 (See legend on next page.)

(See figure on previous page.)

Fig. 2 PTPN20 enhances the metastatic ability of TNBC cells. **(A)** Western blotting demonstrated knockdown of PTPN20 expression following incubation with shRNA targeting PTPN20-3'UTR or PTPN20 plasmids in the MDA-MB-231 and SUM159PT cell lines. GAPDH was used as a loading control. **(B)** Representative micrographs and the percentage of wound closure of the indicated cells by wound healing assay. **(C)** Representative micrographs and quantification of the invasiveness of the indicated cells in the transwell matrix penetration assays. **(D)** Western blotting demonstrated overexpression of PTPN20 following incubation with PTPN20 plasmids in the BT549 and MDA-MB-468 cell lines. GAPDH was used as a loading control. **(E)** Representative micrographs and the percentage of wound closure of indicated cells with overexpression of PTPN20 by wound healing assay. **(F)** Representative micrographs and quantification of the invasiveness of indicated cells with overexpression of PTPN20 in the transwell matrix penetration assays. **(G)** Representative micrographs of tumors in the indicated groups. $n=6$ for each group. **(H)** Tumor volumes were measured on the indicated days in the indicated groups. $n=6$ for each group. **(I)** Average weight of excised tumors from the indicated mice. $n=6$ for each group. **(J)** Lung metastasis burden of xenografted animals was monitored weekly using bioluminescent imaging (BLI). Shown are BLI images of representative mice on day 40 after injection. The color scale depicts the photon flux (photons per second) emitted from the metastasis cells. **(K)** Representative images and H&E staining of lung tissues. Black irregular circles marking the metastatic nodules. Scale bar, 50 μm . **(L)** The metastasis index was calculated (the ratio of lung metastatic nodules number/tumor weight) in the indicated mice. $n=6$ for each group. In (B), (C), (E) and (F), error bars represent the mean \pm SD of three independent experiments. In (B) and (C), Kruskal-Wallis test was used. In (E), (F), (I) and (L), Mann-Whitney U test was used. In (H), One-way repeated-measures ANOVA test was used. *** $P < 0.001$, ** $P < 0.01$, * $P < 0.05$

NF- κ B-dependent gene expression. Moreover, PTPN20 reduced the level of p-p65 Ser468 in a dose-dependent manner (Fig. 3I). We observed that both nuclear and total p65 level was significantly reduced in PTPN20 knockdown groups compared with controls, while overexpression of PTPN20 enhanced nuclear and total expression of p65 (Fig. 3J). The reciprocal immunoprecipitation assays revealed PTPN20 interacted with p65 (Fig. 3K). Phosphorylation of p65 at Ser468 facilitates its binding to COMMD1, a component of a multimeric ubiquitin ligase complex that mediates p65 ubiquitination and degradation. We found that PTPN20 reduced p65 ubiquitination and inhibited the interaction between p65 and COMMD1 (Fig. 3L-M). Collectively, these data demonstrated a key regulatory mechanisms whereby PTPN20 removes phosphorylation of p65 at Ser468 and disrupts the binding of the COMMD1-containing complex to p65, thereby inhibiting p65 ubiquitination and degradation (Fig. 3N).

Downregulation of PTPN20 suppresses the metastasis of TNBC via blocking the p65/NF- κ B signaling

Building on previous findings that PTPN20 promote TNBC cell invasion and migration, we hypothesized that knockdown of PTPN20 inhibits metastatic potential by blocking the p65/NF- κ B pathway. Indeed, reactivation of p65/NF- κ B signaling through p65-S468A mutant transfection markedly increased migratory and invasive capabilities compared to both the PTPN20-shRNA group and the PTPN20-shRNA plus wild-type p65 group (Fig. 4A-D). Additionally, knockdown of PTPN20 reduced the expression levels of TWIST, CSF1, CSF3, CXCL1, IL11 and MMP9, whereas transfection p65-S468A mutant upregulated the expression of NF- κ B target genes (Fig. 4E). Moreover, p65-S468A mutant transfection significantly increased tumor growth rate, tumor weight and lung metastasis burden in PTPN20-silenced tumors (Fig. 4F-K). These results suggested that inhibition of PTPN20 reduces metastatic burden by blocking NF- κ B signaling pathway.

Clinical correlation of PTPN20 with p65 in human TNBC tissues

To further explore the clinical significance of PTPN20 and its subsequent activation of NF- κ B signaling in TNBC tissues, PTPN20 expression and the nuclear p65 levels were examined. PTPN20 and nuclear p65 expression was elevated in metastatic TNBC tissues (T6-10) compared to non-metastatic TNBC tissues (T1-5) (Fig. 5A). Taken together, our results indicated that overexpression of PTPN20 activates NF- κ B signaling by inhibiting p65 phosphorylation at Ser468, thereby promoting TNBC metastasis (Fig. 5B).

Discussion

In summary, these studies suggest that PTPN20 functions as an oncogene to promote TNBC metastasis. We demonstrated that PTPN20 overexpression is associated with the activation NF- κ B signaling pathway. Specifically, PTPN20 inhibits the phosphorylation of p65 and protects it from ubiquitin-mediated degradation via the COMMD1 complex, thereby leading to the activation of NF- κ B signaling pathway. These findings not only enhance our understanding of the molecular mechanisms driving NF- κ B signaling pathway activation and metastasis in breast cancer but also highlight PTPN20 as a potential therapeutic target for TNBC treatment.

Over the past two decades, extensive research on triple-negative breast cancer (TNBC) has led to the development of novel therapeutic options, including immune checkpoint inhibitors, PARP inhibitors, antibody-drug conjugates (ADCs), and other promising agents and combinations [34–36]. Unfortunately, the extent of response duration of these novel options was limited and the improvement of survival was barely satisfied, and chemotherapy remains the mainstay treatment option of TNBC. Disease progression and distant metastasis post-systemic treatment remain the unsolved challenge and life threatening issues in TNBC patients. Understanding the mechanisms underlying distant metastasis is crucial for

developing strategies to reduce metastasis and improve overall survival. Our study identified the phosphatase PTPN20 as an oncogenic factor that promotes metastasis in TNBC by activating the NF- κ B signaling pathway, suggesting that PTPN20 may be a promising therapeutic target for TNBC treatment.

Hyperactivation of NF- κ B signal pathway plays a pivotal role in tumor progression and distant metastasis in breast cancer [37]. Therefore, understanding the stimuli of NF- κ B activation as well as the regulatory mechanisms helps to identify potential targets to block the aberrant NF- κ B pathway and retard tumor progression. While many post-translational modifications (PTMs) were found to regulate the IKK complex and I κ B proteins, there existed other important PTMs in the NF- κ B subunits [20]. p65 forms the most abundant form of activated NF- κ B. Several sites of phosphorylation have been identified, which induces a conformational change, and subsequently impacts p65 activation, stability, and protein interaction. Taken together, our results uncover a plausible mechanism underlying the intrinsic metastatic property of TNBC and might represent an attractive therapeutic target in the treatment of TNBC.

An increasing number of p65 phosphorylation sites have been identified such as Ser468, Ser529 and Ser536 [38–41]. The phosphorylation of p65 at different sites may lead to different consequences. As previous report, the expression of p-p65 Ser529 increased rapidly following stimulation and that nuclear localization of p-p65 Ser529 followed the nuclear localization pattern of total p65 [39]. Besides, p-Ser536 also promotes nuclear translocation of p65 [42]. Moreover, basal Ser468 phosphorylation, which is contained in a carboxy-terminal transactivation domain, is regulated by glycogen synthase kinase 3 [43], whereas stimulus-induced modification is mediated by I κ B kinase (IKK)- β and IKK ϵ [44]. Importantly, p-p65 Ser468 was found to be ubiquitinated and degraded in the nucleus, thus allowing termination of the nuclear NF- κ B response [21, 22]. Phosphorylation at S468 in the transactivation domain 2 (TAD2) of p65 was found to terminate activated p65 which interact with chromatin in the nucleus, by recruiting an E3 ligase COMMD1, cullin2, leading to the ubiquitination and subsequent proteasomal degradation of p65 [21, 45]. The dynamic regulation of p65

dephosphorylation and phosphorylation modulates NF- κ B signaling under diverse conditions, influencing cancer metastasis, immune responses, and other outcomes. Although the kinases involved in NF- κ B phosphorylation are well-characterized, the phosphatases responsible for its dephosphorylation remain largely unexplored. Our study showed that PTPN20 acted as a bona-fide phosphatase targeting Ser468 of p65. By binding to and dephosphorylating p65 at Ser468, PTPN20 decreased p65 degradation and enhanced the expression of downstream genes of NF- κ B. Overexpression of PTPN20 promoted tumor progression and distant metastasis in breast cancer, while knockdown of PTPN20 dramatically eliminated NF- κ B signaling in breast cancer and inhibited tumor growth and metastasis. Of note, PTPN20 was not found to dephosphorylate Ser536 in the transactivation domain (TAD) of p65, which is critical for its transcriptional activity, suggesting that PTPN20 selectively dephosphorylates p65 to enhance NF- κ B activity.

The Protein Tyrosine Phosphatases (PTP) superfamily contains more than 100 members, and much less is known about the role of PTPN20 in tumor progression. To date, a study has identified that PTPN20 levels is associated with immune cell infiltration and tumor mutation burden in gastric cancer patients [28]. Besides, a variant of human PTPN20, PTPN20A, is expressed in a wide range of both normal and transformed cell lines and associated with a dynamic subcellular distribution that is targeted to sites of actin polymerization [46]. But whether these effects are based on phosphatase activity of PTPN20 and the corresponding mechanism remain unclear. In the present study, we found a direct association between PTPN20 and p65. Inhibition of PTPN20 by siRNA technique significantly increased p65 phosphorylation and protect p65 from ubiquitin-mediated degradation. Furthermore, whether PTPN20 could be involved in NF- κ B pathway due to nuclear translocation of PTPN20 remains further studied. Given the pro-metastatic potential of PTPN20, further investigation into its expression and role in other cancers will offer valuable insights into the mechanisms driving metastasis. Additionally, these studies may pave the way for the development of novel therapeutic strategies for the treatment of human cancers.

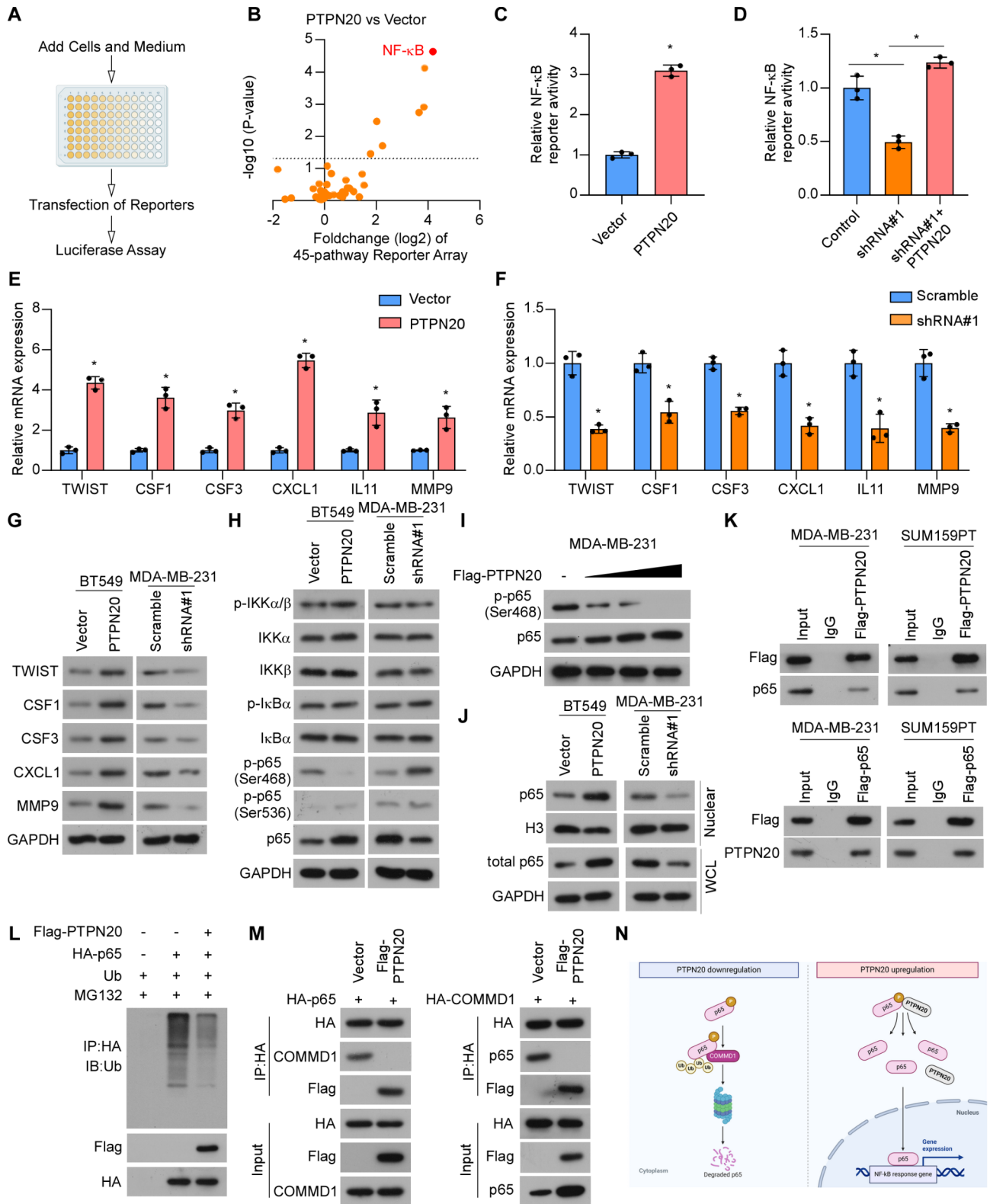


Fig. 3 (See legend on next page.)

(See figure on previous page.)

Fig. 3 PTPN20 activates p65/NF- κ B signaling pathway in TNBC cells. **(A-B)** Signal finder signal transduction 45-pathway reporter array showing that PTPN20 overexpression significantly activated NF- κ B signaling in MDA-MB-231 cells. **(C-D)** Relative NF- κ B-driven Luciferase activity was analyzed in the indicated cells. **(E-F)** Real-time PCR analysis of downstream NF- κ B pathway target genes mRNA levels in the indicated cells. **(G)** Western blotting analysis of downstream NF- κ B pathway target genes protein levels in the indicated cells. GAPDH was used as a loading control. **(H)** Western blotting analysis of levels of p-IKK α / β , IKK α , IKK β , p-I κ B α , I κ B α , p-p65 (Ser468), p-p65 (Ser536) and total p65 in the indicated cells. GAPDH was used as a loading control. **(I)** Western blotting analysis of level of p-p65 (Ser468) in the cells transfected with PTPN20 plasmid (0 μ g, 0.5 μ g, 1 μ g and 2 μ g). GAPDH was used as a loading control. **(J)** Western blotting analysis of level of nuclear p65 and total p65 in the indicated cells. H3, Histone 3. GAPDH was used as a loading control. **(K)** Total cell lysates from MDA-MB-231 cells and SUM159PT cells were immunoprecipitated with anti-Flag antibody in the indicated cells. The immunoprecipitates were subjected to immunoblotting analysis with anti-p65 or anti-PTPN20 to detect interaction. **(L)** Total cell lysates were immunoprecipitated with anti-HA antibody in the indicated cells. The immunoprecipitates were subjected to immunoblotting analysis with anti-Ub, anti-Flag and anti-HA. **(M)** Total cell lysates from MDA-MB-231 cells were immunoprecipitated with anti-HA antibody. The immunoprecipitates were subjected to immunoblotting analysis with indicated antibodies to detect interaction between COMMD1 and p65. **(N)** Hypothetical model illustrating that PTPN20 dephosphorylates and stabilizes p65 by inhibiting the combination between p65 and COMMD1, leading to NF- κ B activation (Created in BioRender.com). In (C), (D), (E) and (F), error bars represent the mean \pm SD of three independent experiments. In (C), (E) and (F), Mann-Whitney U test was used. In (D), Kruskal-Wallis test was used. *** $P < 0.001$, ** $P < 0.01$, * $P < 0.05$

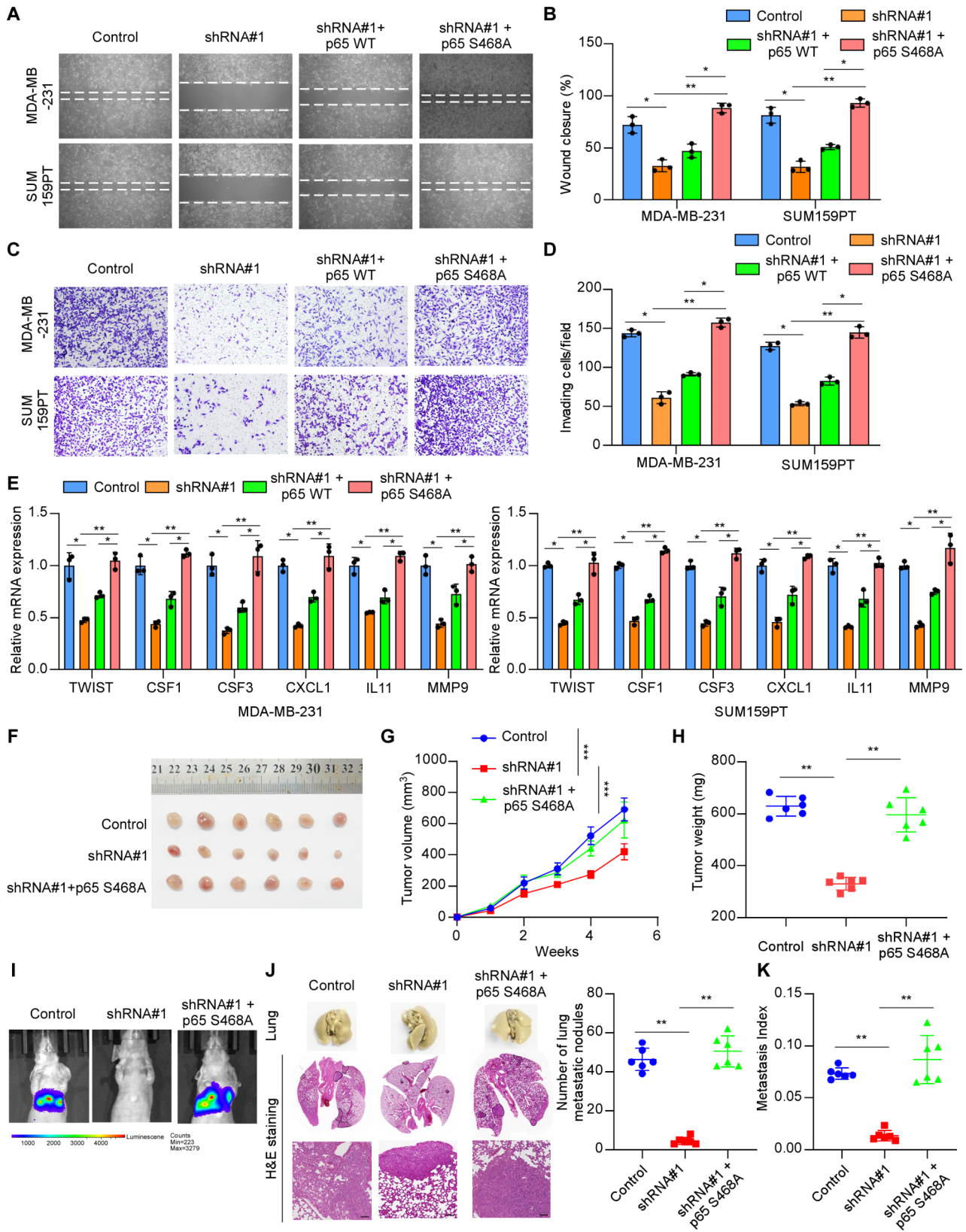


Fig. 4 (See legend on next page.)

(See figure on previous page.)

Fig. 4 Downregulation of PTPN20 suppresses the metastasis of TNBC via blocking the p65/NF- κ B signaling. **(A-B)** Representative micrographs and the percentage of wound closure of indicated cells by wound healing assay. **(C-D)** Representative micrographs and quantification of the invasiveness of indicated cells in the transwell matrix penetration assays. **(E)** Real-time PCR analysis of downstream NF- κ B pathway target genes mRNA levels in the indicated cells. **(F)** Representative micrographs of tumors in the indicated groups. $n=6$ for each group. **(G)** Tumor volumes were measured on the indicated days in the indicated groups. $n=6$ for each group. **(H)** Average weight of excised tumors from the indicated mice. $n=6$ for each group. **(I)** Lung metastasis burden of xenografted animals was monitored weekly using bioluminescent imaging (BLI). Shown are BLI images of representative mice on day 40 after injection. **(J)** Representative images and H&E staining of lung tissues. Black irregular circles marking the metastatic nodules. Scale bar, 50 μ m. Quantification of lung metastatic nodules numbers was shown (right). **(K)** The metastasis index was calculated (the ratio of lung metastatic nodules number/tumor weight) in the indicated mice. $n=6$ for each group. In (B), (D) and (E), error bars represent the mean \pm SD of three independent experiments. In (B), (D), (E), (H), (J) and (K), Kruskal-Wallis test was used. In (G), One-way repeated-measures ANOVA test was used. *** $P < 0.001$, ** $P < 0.01$, * $P < 0.05$

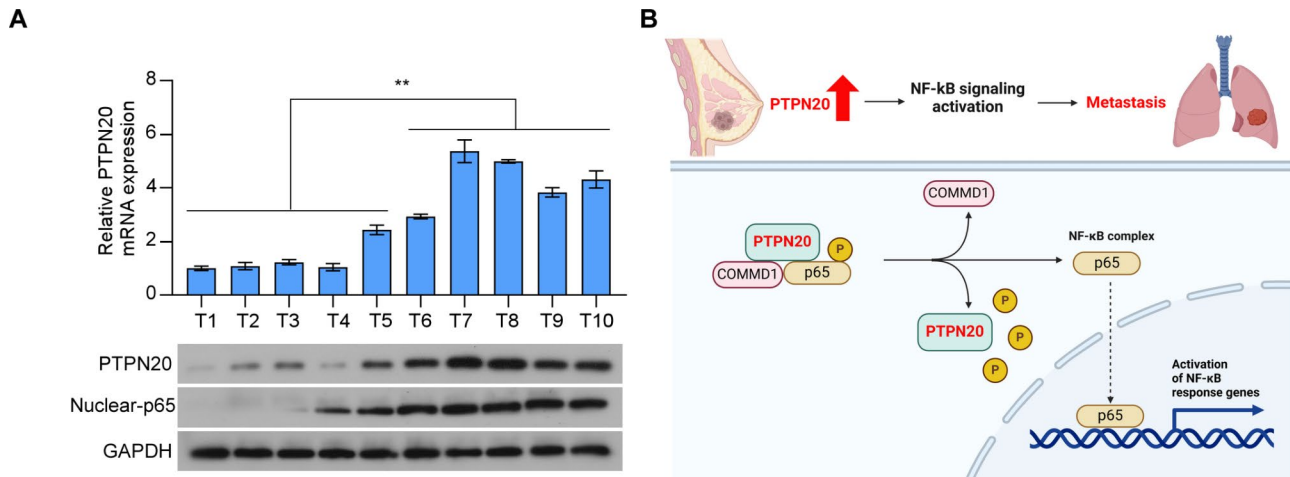


Fig. 5 Clinical correlation of PTPN20 with p65 in human TNBC tissues. **(A)** Real-time PCR (up) and western blotting (down) analysis of PTPN20 expression in 5 non-metastatic TNBC tissues and 5 metastatic TNBC tissues. **(B)** Hypothetical model illustrating that the activation of NF- κ B by PTPN20 promotes metastasis in TNBC (Created in BioRender.com). In (A), error bars represent the mean \pm SD of three independent experiments, Mann-Whitney U test was used. *** $P < 0.001$, ** $P < 0.01$, * $P < 0.05$

Conclusions

Extensive research on TNBC has led to novel therapies, yet limited response duration and modest survival improvements keep chemotherapy as the main treatment. Our study identifies PTPN20 as an oncogenic phosphatase that promotes metastasis by selectively dephosphorylating Ser468 of p65, enhancing NF- κ B signaling. Overexpression of PTPN20 facilitates tumor growth and metastasis, while its knockdown inhibits these processes. Given its pro-metastatic role, further exploration of PTPN20 in other cancers may reveal new therapeutic strategies to combat cancer progression.

Supplementary Information

The online version contains supplementary material available at <https://doi.org/10.1186/s13058-024-01910-w>.

Supplementary Material 1

Acknowledgements

Not applicable.

Author contributions

XX.Z., XH.Z., XF.Z., and QY.L. carried out most of the experimental work; they collected and analyzed the data. XY.J., SM.H., XW.C., and XF.C. conducted the Real-time PCR and western blotting. XX.Z., XH.Z., and XF.Z. collected tissues and patient information, conducted IHC and survival analysis. XX.Z., XH.Z., XF.Z., and QY.L. conducted the plasmid constructions and IP assays. XX.Z., SM.H., XW.C., and XF.C. conducted animal studies. WH.J. provided technical support for data analysis. XH.Z. conducted cell culture and performed the in vitro studies. XX.Z., XH.Z., XF.Z., QY.L., HQ.Z., DN.S., and XK.Q. raised the concept, design the experiments, wrote the manuscript, and supervised the project. HQ.Z., DN.S., and XK.Q. gave the valuable guidance on this article. All authors reviewed the manuscript. The order of the co-first authors was assigned based on their efforts and contributions to the study.

Funding

This work was supported by Medical Science and Technology Research Program of Henan Province (LHGJ20190025), National Natural Science Foundation of China (No.82303157), China Postdoctoral Science Foundation (No.2023M734041), China Postdoctoral Innovation Talent Support Program (No.BX20230441).

Data availability

No datasets were generated or analysed during the current study.

Declarations

Ethics approval and consent to participate

Ethics approval (No. B2024-053) and prior patient consents were obtained from the Institutional Research Ethics Committee of Sun Yat-sen University Cancer Center to use the clinical specimens for research purposes. Animal experimental procedures were approved by the Institutional Animal Care and Use Committee of Sun Yat-sen University (No. L102042024000K). According to the guidelines (GB/T35892-2018), the ethics committee specified that the maximal tumor burden is no more than 10% of the body weight of animals and the average diameter is less than 20 mm. During the experiment, the tumor sizes of the mice complied with the regulations. The study complied with the principles set out in the Declaration of Helsinki.

Consent for publication

Not applicable.

Competing interests

The authors declare no competing interests.

Corresponding authors

Correspondence to Hequn Zou, Dongni Shi or Xueke Qian.

Author details

¹Department of Breast Surgery, The First Affiliated Hospital of Zhengzhou University, Zhengzhou, Henan 450052, China

²Department of Experimental Research, State Key Laboratory of Oncology in South China, Collaborative Innovation Center for Cancer Medicine, Sun Yat-sen University Cancer Center, Guangzhou, Guangdong 510060, China

³Department of Radiotherapy, The First Affiliated Hospital of Zhengzhou University, Zhengzhou, Henan 450052, China

⁴Department of Oncology, The First Affiliated Hospital of Zhengzhou University, Zhengzhou, Henan 450052, China

⁵School of Medicine, The Chinese University of Hong Kong, Shenzhen, Guangdong 518172, China

⁶Department of Biochemistry, Zhongshan School of Medicine, Sun Yat-sen University, Guangzhou, Guangdong 510080, China

⁷Department of Biobank, State Key Laboratory of Oncology in South China, Collaborative Innovation Center for Cancer Medicine, Sun Yat-sen University Cancer Center, Guangzhou, Guangdong 510060, China

Received: 22 July 2024 / Accepted: 22 October 2024

Published online: 06 November 2024

References

- Bray F, Ferlay J, Soerjomataram I, Siegel RL, Torre LA, Jemal A. <ArticleTitle Language="En">Global cancer statistics 2018: GLOBOCAN estimates of incidence and mortality worldwide for 36 cancers in 185 countries. *Cancer J Clin*. 2018;68(6):394–424.
- Brown M, Tsodikov A, Bauer KR, Parise CA, Caggiano V. The role of human epidermal growth factor receptor 2 in the survival of women with estrogen and progesterone receptor-negative, invasive breast cancer: the California Cancer Registry, 1999–2004. *Cancer*. 2008;112(4):737–47.
- Garrido-Castro AC, Lin NU, Polyak K. Insights into Molecular Classifications of Triple-Negative Breast Cancer: Improving Patient Selection for Treatment. *Cancer Discov*. 2019;9(2):176–98.
- Carey LA, Perou CM, Livasy CA, Dressler LG, Cowan D, Conway K, et al. Race, breast cancer subtypes, and survival in the Carolina Breast Cancer Study. *JAMA*. 2006;295(21):2492–502.
- Loibl S, Poortmans P, Morrow M, Denkert C, Curigliano G. Breast cancer. *Lancet (London England)*. 2021;397(10286):1750–69.
- Kassam F, Enright K, Dent R, Dranitsaris G, Myers J, Flynn C, et al. Survival outcomes for patients with metastatic triple-negative breast cancer: implications for clinical practice and trial design. *Clin Breast Cancer*. 2009;9(1):29–33.
- Foulkes WD, Smith IE, Reis-Filho JS. Triple-negative breast cancer. *N Engl J Med*. 2010;363(20):1938–48.
- Yin L, Duan JJ, Bian XW, Yu SC. Triple-negative breast cancer molecular subtyping and treatment progress. *Breast cancer research: BCR*. 2020;22(1):61.
- Li Y, Zhang H, Merkher Y, Chen L, Liu N, Leonov S, et al. Recent advances in therapeutic strategies for triple-negative breast cancer. *J Hematol Oncol*. 2022;15(1):121.
- Labelle M, Begum S, Hynes RO. Direct signaling between platelets and cancer cells induces an epithelial-mesenchymal-like transition and promotes metastasis. *Cancer Cell*. 2011;20(5):576–90.
- Zhang M, Liu ZZ, Aoshima K, Cai WL, Sun H, Xu T, et al. CECR2 drives breast cancer metastasis by promoting NF- κ B signaling and macrophage-mediated immune suppression. *Sci Transl Med*. 2022;14(630):eabf5473.
- Park BK, Zhang H, Zeng Q, Dai J, Keller ET, Giordano T, et al. NF- κ B in breast cancer cells promotes osteolytic bone metastasis by inducing osteoclastogenesis via GM-CSF. *Nat Med*. 2007;13(1):62–9.
- Wan F, Lenardo MJ. The nuclear signaling of NF- κ B: current knowledge, new insights, and future perspectives. *Cell Res*. 2010;20(1):24–33.
- Sen R, Baltimore D. Inducibility of kappa immunoglobulin enhancer-binding protein NF- κ B by a posttranslational mechanism. *Cell*. 1986;47(6):921–8.
- Urban MB, Schreck R, Baeuerle PA. NF- κ B contacts DNA by a heterodimer of the p50 and p65 subunit. *EMBO J*. 1991;10(7):1817–25.
- Hinz M, Scheidereit C. The I κ B kinase complex in NF- κ B regulation and beyond. *EMBO Rep*. 2014;15(1):46–61.
- Yu H, Lin L, Zhang Z, Zhang H. Targeting NF- κ B pathway for the therapy of diseases: mechanism and clinical study. *Signal Transduct Target therapy*. 2020;5(1):209.
- Yeung F, Hoberg JE, Ramsey CS, Keller MD, Jones DR, Frye RA, et al. Modulation of NF- κ B-dependent transcription and cell survival by the SIRT1 deacetylase. *EMBO J*. 2004;23(12):2369–80.
- Häcker H, Karin M. Regulation and function of IKK and IKK-related kinases. *Science's STKE: signal Transduct Knowl Environ*. 2006;2006(357):re13.
- Jacque E, Tchenio T, Piton G, Romeo PH, Baud V. RelA repression of RelB activity induces selective gene activation downstream of TNF receptors. *Proc Natl Acad Sci USA*. 2005;102(41):14635–40.
- Ryo A, Suizu F, Yoshida Y, Perrem K, Liou YC, Wulf G, et al. Regulation of NF- κ B signaling by Pin1-dependent prolyl isomerization and ubiquitin-mediated proteolysis of p65/RelA. *Mol Cell*. 2003;12(6):1413–26.
- Carmody RJ, Ruan Q, Palmer S, Hilliard B, Chen YH. Negative regulation of toll-like receptor signaling by NF- κ B p50 ubiquitination blockade. *Sci (New York NY)*. 2007;317(5838):675–8.
- Manguso RT, Pope HW, Zimmer MD, Brown FD, Yates KB, Miller BC, et al. In vivo CRISPR screening identifies Ptpn2 as a cancer immunotherapy target. *Nature*. 2017;547(7664):413–8.
- Cai J, Huang S, Yi Y, Bao S. Downregulation of PTPN18 can inhibit proliferation and metastasis and promote apoptosis of endometrial cancer. *Clin Exp Pharmacol Physiol*. 2019;46(8):734–42.
- Tang X, Qi C, Zhou H, Liu Y. Critical roles of PTPN family members regulated by non-coding RNAs in tumorigenesis and immunotherapy. *Front Oncol*. 2022;12:972906.
- Zhang Z, Christin JR, Wang C, Ge K, Oktay MH, Guo W. Mammary-Stem-Cell-Based Somatic Mouse Models Reveal Breast Cancer Drivers Causing Cell Fate Dysregulation. *Cell Rep*. 2016;16(12):3146–56.
- Chen J, Zhao X, Yuan Y, Jing JJ. The expression patterns and the diagnostic/prognostic roles of PTPN family members in digestive tract cancers. *Cancer Cell Int*. 2020;20:238.
- Ma L, Liu Y, Wang Y, Yang J, Lu J, Feng H, et al. Identification of PTPN20 as an innate immunity-related gene in gastric cancer with *Helicobacter pylori* infection. *Front Immunol*. 2023;14:1212692.
- Xu H, Miyajima M, Nakajima M, Ogino I, Kawamura K, Akiba C, et al. Ptpn20 deletion in H-Tx rats enhances phosphorylation of the NKCC1 cotransporter in the choroid plexus: an evidence of genetic risk for hydrocephalus in an experimental study. *Fluids barriers CNS*. 2022;19(1):39.
- Saal LH, Vallon-Christersson J, Häkkinen J, Hegardt C, Grabau D, Winter C, et al. The Sweden Cancerome Analysis Network - Breast (SCAN-B) Initiative: a large-scale multicenter infrastructure towards implementation of breast cancer genomic analyses in the clinical routine. *Genome Med*. 2015;7(1):20.
- Brueffer C, Vallon-Christersson J, Grabau D, Ehinger A, Häkkinen J, Hegardt C et al. Clinical Value of RNA Sequencing-Based Classifiers for Prediction of the Five Conventional Breast Cancer Biomarkers: A Report From the Population-Based Multicenter Sweden Cancerome Analysis Network-Breast Initiative. *JCO precision Oncol* 2018;2.
- Lehmann BD, Bauer JA, Chen X, Sanders ME, Chakravarthy AB, Shyr Y, et al. Identification of human triple-negative breast cancer subtypes and preclinical models for selection of targeted therapies. *J Clin Investig*. 2011;121(7):2750–67.
- Bottoni L, Minetti A, Realini G, Pio E, Giustarini D, Rossi R, et al. NRF2 activation by cysteine as a survival mechanism for triple-negative breast cancer cells. *Oncogene*. 2024;43(22):1701–13.
- Dri A, Arpino G, Bianchini G, Curigliano G, Danesi R, De Laurentiis M, et al. Breaking barriers in triple negative breast cancer (TNBC) - Unleashing the power of antibody-drug conjugates (ADCs). *Cancer Treat Rev*. 2024;123:102672.
- Vojtek M, Marques MPM, Ferreira I, Mota-Filipe H, Diniz C. Anticancer activity of palladium-based complexes against triple-negative breast cancer. *Drug Discovery Today*. 2019;24(4):1044–58.
- Bianchini G, Balko JM, Mayer IA, Sanders ME, Gianni L. Triple-negative breast cancer: challenges and opportunities of a heterogeneous disease. *Nat reviews Clin Oncol*. 2016;13(11):674–90.
- Mohan S, Hakami MA, Dailah HG, Khalid A, Najmi A, Zoghebi K, et al. From inflammation to metastasis: The central role of miR-155 in modulating NF- κ B in cancer. *Pathol Res Pract*. 2024;253:154962.
- Mattioli I, Geng H, Sebald A, Hodel M, Bucher C, Kracht M, et al. Inducible phosphorylation of NF- κ B p65 at serine 468 by T cell costimulation is mediated by IKK epsilon. *J Biol Chem*. 2006;281(10):6175–83.
- Maguire O, O'Loughlin K, Minderman H. Simultaneous assessment of NF- κ B/p65 phosphorylation and nuclear localization using imaging flow cytometry. *J Immunol Methods*. 2015;423:3–11.
- Chien CS, Li JY, Chien Y, Wang ML, Yarmishyn AA, Tsai PH et al. METTL3-dependent N(6)-methyladenosine RNA modification mediates the atherogenic inflammatory cascades in vascular endothelium. *Proc Natl Acad Sci USA* 2021;118(7).
- Yde CW, Emdal KB, Guerra B, Lykkesfeldt AE. NF κ B signaling is important for growth of antiestrogen resistant breast cancer cells. *Breast Cancer Res Treat*. 2012;135(1):67–78.
- Bijli KM, Fazal F, Rahman A. Regulation of RelA/p65 and endothelial cell inflammation by proline-rich tyrosine kinase 2. *Am J Respir Cell Mol Biol*. 2012;47(5):660–8.

43. Buss H, Dörrie A, Schmitz ML, Frank R, Livingstone M, Resch K, et al. Phosphorylation of serine 468 by GSK-3beta negatively regulates basal p65 NF-kappaB activity. *J Biol Chem*. 2004;279(48):49571–4.
44. Schwabe RF, Sakurai H. IKKbeta phosphorylates p65 at S468 in transactivaton domain 2. *FASEB journal: official publication Federation Am Soc Experimental Biology*. 2005;19(12):1758–60.
45. Tanaka T, Grusby MJ, Kaisho T. PDLIM2-mediated termination of transcription factor NF-kappaB activation by intranuclear sequestration and degradation of the p65 subunit. *Nat Immunol*. 2007;8(6):584–91.
46. Fodero-Tavoletti MT, Hardy MP, Cornell B, Katsis F, Sadek CM, Mitchell CA, et al. Protein tyrosine phosphatase hPTPN20a is targeted to sites of actin polymerization. *Biochem J*. 2005;389(Pt 2):343–54.

Publisher's note

Springer Nature remains neutral with regard to jurisdictional claims in published maps and institutional affiliations.